

Quantum Dot Spectroscopy Using Cavity Quantum Electrodynamics

Martin Winger,^{1,*} Antonio Badolato,¹ Kevin J. Hennessy,^{1,2} Evelyn L. Hu,² and Ataç Imamoglu¹

¹*Institute of Quantum Electronics, ETH Zurich, 8093 Zurich, Switzerland*

²*California NanoSystems Institute, University of California, Santa Barbara, California 93106, USA*

(Received 3 September 2008; published 25 November 2008)

We show how cavity quantum electrodynamics using a tunable photonic crystal nanocavity in the strong-coupling regime can be used for single quantum dot spectroscopy. From the distinctive avoided crossings observed in the strongly coupled system we can identify the neutral and single positively charged exciton as well as the biexciton transitions. Moreover we are able to investigate the fine structure of those transitions and to identify a novel cavity mediated mixing of bright and dark exciton states, where the hyperfine interactions with lattice nuclei presumably play a key role. These results are enabled by a deterministic coupling scheme which allowed us to achieve unprecedented coupling strengths in excess of $150 \mu\text{eV}$.

DOI: [10.1103/PhysRevLett.101.226808](https://doi.org/10.1103/PhysRevLett.101.226808)

PACS numbers: 73.21.La, 42.50.Pq, 42.70.Qs, 68.65.Hb

Cavity quantum electrodynamics (QED) studies the quantum limit of light-matter interaction in an optical cavity [1]; its implementation in both atomic [2] and solid state systems [3] has received substantial interest primarily due to potential applications in quantum information processing [1,4]. Self-assembled quantum dots (QDs) embedded in monolithic nanocavities provide a well-controlled and robust system for conducting cavity QED experiments in the solid state. The combination of ultra-small mode volumes and high Q values provided by those systems has made it possible to enter the strong-coupling regime of cavity QED with different types of monolithic cavities [5–8]. However, in all previously reported experiments, a nanocavity mode was brought into resonance with a QD transition whose nature has not been specified. This is mainly due to the fact that the inherently random excitation scheme used in photoluminescence (PL) spectroscopy allows for the creation of a multitude of QD charge configurations and the resulting spectral emission lines are generally difficult to interpret. This ambiguity has not hindered progress in the field, since the emphasis has so far been on using the QD as a two-level emitter that couples resonantly to a nanocavity mode [9,10]; the nature of the particular QD transition was irrelevant for the study of cavity QED physics.

In contrast, we show here that a nanocavity mode that is strongly coupled to QD transitions can be used as a powerful spectroscopic tool for studying fundamental properties of the QD itself. The distinct spectral anticrossings observed when the cavity is tuned across resonance with different QD transitions allow us first of all to unambiguously identify the single (positively) charged exciton (X^+), the neutral exciton (X^0), and the neutral biexciton (XX^0) emission lines. Surprisingly, cavity QED also allows us to study the fine structure of QD transitions and identify a novel strong-coupling induced mixing of bright and dark exciton complexes.

In order to reach the strong-coupling regime the coherent coupling g between an excitonic transition and a cavity field has to exceed the decay rates of the exciton (Γ) and the cavity (κ), obeying $g > \Gamma/4, \kappa/4$ [11]. This is achieved in a deterministic fashion using the approach introduced in [8,12] where cavities are precisely positioned around pre-selected QDs in order to achieve maximum coupling. InAs QDs were grown by molecular beam epitaxy in the center of a 126 nm thick GaAs membrane on top of a 1 μm thick $\text{Al}_{0.7}\text{Ga}_{0.3}\text{As}$ layer that allowed for subsequent cavity membrane formation. We identified well-isolated QDs in PL and mapped them by atomic force microscopy. Around those QDs we fabricated photonic crystal (PC) defect cavities in the $L3$ configuration [13] using electron beam lithography in combination with a dry and wet etching process. The device we study here has negligible misalignment between the QD and the field maximum of the first order cavity mode, such that we expect maximum coupling g .

The micro-PL studies were carried out at $T = 4.2 \text{ K}$ using a liquid helium flow cryostat. The laser beam used for off-resonant excitation was focused onto the PC cavity using a microscope objective with a numerical aperture of $\text{NA} = 0.55$. The luminescence signal was collected with the same microscope objective, coupled into a single mode fiber, and directed to a grating spectrometer with a spectral resolution of $30 \mu\text{eV}$. Moreover, a polarizer in the detection path allowed for doing polarization-sensitive PL measurements.

In the lowest energy conduction band states of a QD, electrons have spin z component $S_{e,z} = \pm \frac{1}{2}$, while the (heavy) holes in the lowest energy valence-band states carry pseudospin $J_{h,z} = \pm \frac{3}{2}$ [14]. The total angular momentum projection of the lowest energy electron-hole pairs (excitons) therefore can take the values $M = \pm 1, \pm 2$. The $M = \pm 2$ states (dark excitons) cannot recombine optically, since their decay requires an angular momentum transfer

of $2\hbar$, while the $M = \pm 1$ states give rise to the X^0 luminescence. The electron-hole exchange interaction has the effect of (i) splitting dark and bright states by $\delta_0 \sim 100\text{--}200 \mu\text{eV}$ and (ii) lifting the degeneracy of both bright and dark manifolds [14–16]. The coupled excitonic eigenstates then are $|D_{a,b}\rangle = (|+2\rangle \pm |-2\rangle)/\sqrt{2}$ for the dark exciton doublet and $|X_{x,y}^0\rangle = (|+1\rangle \pm |-1\rangle)/\sqrt{2}$ for the bright doublet [Fig. 1(a)]. The latter decay by emitting photons that are linearly polarized along either of the two QD axes (x, y).

The cavity mode electric field in the center of the PC defect, i.e., at the location of the QD, is oriented along the y direction (perpendicular to the $L3$ defect line). Therefore we assume maximum coupling g between the cavity single-photon state $|g, 1_c\rangle$ and $|X_y^0, 0_c\rangle$; the second bright exciton state $|X_x^0, 0_c\rangle$ is not coupled to the cavity. This is schematized in Fig. 1(b) where the dressed QD-cavity states are shown for the cavity on resonance with $|X_y^0, 0_c\rangle$. While the uncoupled state $|X_x^0, 0_c\rangle$ remains unchanged, $|X_y^0, 0_c\rangle$ hybridizes with $|g, 1_c\rangle$, thereby forming the polariton states $|p_{\pm}\rangle = (|X_y^0, 0_c\rangle \pm |g, 1_c\rangle)/\sqrt{2}$.

The inset in Fig. 2 shows a typical PL spectrum for a pump wavelength of $\lambda_{\text{ex}} = 818 \text{ nm}$ and a pump power of $P_{\text{ex}} = 10 \text{ nW}$. We assign the line denoted with X^0 to spontaneous recombination of the states $|X_x^0, 0_c\rangle$ and $|X_y^0, 0_c\rangle$, which are typically split by $0\text{--}30 \mu\text{eV}$. In the particular QD we study here, this splitting lies below the resolution of our spectral apparatus. The identification of this line as X^0 becomes obvious in the results presented below. Moreover we tentatively assign the line denoted by X^+ to emission from the positively charged exciton, where in addition to the electron-hole pair an extra hole is trapped within the QD. The splitting of 0.5 nm from the X^0 is in agreement with previous studies of similar QDs. We remark here that in order to obtain the shown PL spectrum we had to carefully study the pump-wavelength dependence of the PL: clear emission from the X^0 and X^+ is only present for a limited range of pump laser wavelengths.

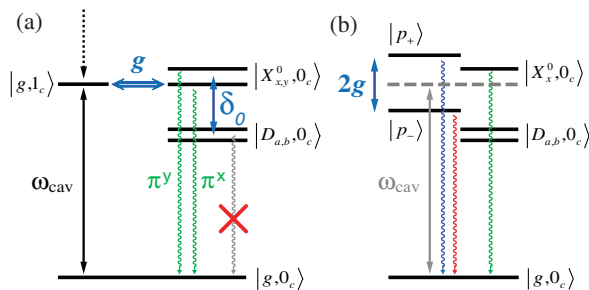


FIG. 1 (color). X^0 level scheme. (a) QD eigenstates and the cavity mode one-photon state. (b) As the cavity electric field vector is parallel to the y direction at the QD, coherent coupling g occurs with $|X_y^0, 0_c\rangle$, giving rise to the polariton states $|p_{\pm}\rangle$, while $|X_x^0, 0_c\rangle$ is not influenced by the cavity mode.

The peak around 931.5 nm corresponds to emission from the uncoupled cavity mode. This feature exhibits a Lorentzian line shape with a Q factor of 16000 ($\kappa = 83 \mu\text{eV}$) and is predominantly polarized along the y direction (degree of polarization = 96%). As has been shown in our previous work, efficient cavity mode emission is always present, irrespective of the detuning from QD spectral features [8]. Photon cross-correlation measurements revealed that this emission is solely due to the presence of a single QD in the PC membrane.

In order to tune the cavity mode into resonance with the QD excitons, we employed a thin film gas-deposition technique to continuously redshift the cavity mode wavelength [10,17]. Figure 2 shows PL data for different cavity mode wavelengths in a color plot. For each recorded spectrum, the central wavelength of the (uncoupled) cavity mode has been extracted and used to linearize the vertical axis. Furthermore, since the total intensity of the spectra fluctuates in time as a result of sample drift, each spectrum has been normalized to its integral. In the data shown here, the polarizer was oriented along the y direction in order to maximize the signal from the cavity mode. As we cross the shorter wavelength line (X^+), we observe an anticrossing of the cavity and QD lines along with a central peak that corresponds to emission from the uncoupled cavity mode at times when the QD occupies a charging state other than the X^+ . The vacuum Rabi splitting is found to be $2g = 205 \mu\text{eV}$. The strong-coupling condition $g > \kappa/4, \Gamma/4$ is obviously well fulfilled for those parameter values. Moreover, we observe that the emission of the strongly coupled polariton doublet is copolarized with the cavity mode.

As gas tuning proceeds, the cavity moves into resonance with the X^0 peak in the spectrum. The two anticrossing

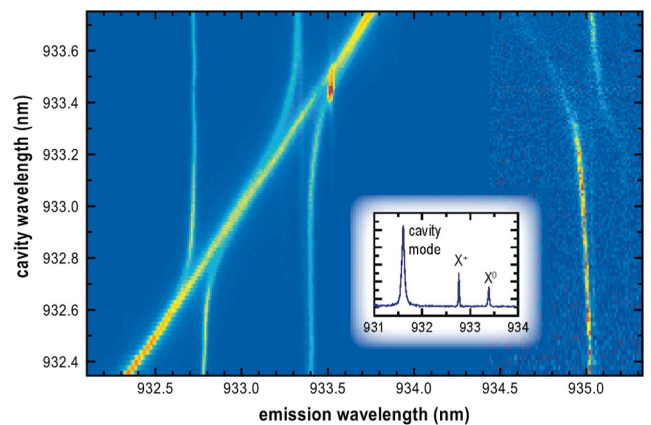


FIG. 2 (color). PL color plot when tuning the cavity mode across the X^+ and X^0 transitions. For both lines a clear anticrossing can be observed. The inset shows a typical PL spectrum for the cavity blue detuned from the X^+ line. For wavelengths on the red side of 934.5 nm the color scale has been offset by a factor of 26 in order to highlight the biexciton emission.

lines here correspond to emission from the polariton states $|p_{\pm}\rangle$ that here show a vacuum Rabi splitting of $2g = 316 \mu\text{eV}$, which is, to the best of our knowledge, the largest splitting reported so far in any cavity QED system with a single emitter. The approximately 1.5 times larger coupling to this peak compared to the one observed with the X^+ line is consistent with our identification of this peak with the X^0 line and arises from the fact that the X^+ trion transitions are circularly polarized.

Furthermore, we observe that the neutral biexciton line XX^0 at $\lambda_{XX^0} = 935 \text{ nm}$ undergoes a splitting as the cavity is on resonance with the X^0 , which can be seen as the anticrossing feature around that wavelength in Fig. 2. Since the pump power here is well below the saturation of the QD, emission from the XX^0 is rather weak. For this reason the color scale of Fig. 2 has been normalized for wavelengths longer than 934.5 nm . Since the XX^0 emission arises from biexciton decay to the neutral exciton states $|X_{x,y}^0\rangle$, the vacuum Rabi splitting of $|X_y^0\rangle$ leads to a splitting of the XX^0 line. The upper (lower) polariton state shifts the biexciton decay to lower (higher) emission energy; therefore, the anticrossing feature of XX^0 appears horizontally flipped with respect to that of the X^0 . Since the PL shown here is y polarized, the unsplit XX^0 emission to the $|X_x^0\rangle$ state is not observable.

The splitting of the two anticrossing XX^0 branches amounts to 0.22 nm , identical to the vacuum Rabi splitting of the X^0 itself. Moreover, the intensity of the cavitylike branches decays when moving away from resonance. This is exactly the behavior expected from the XX^0 decaying to the QD-like component of the intermediate polariton states $|p_{\pm}\rangle$. Furthermore, we note that there is no signature of an

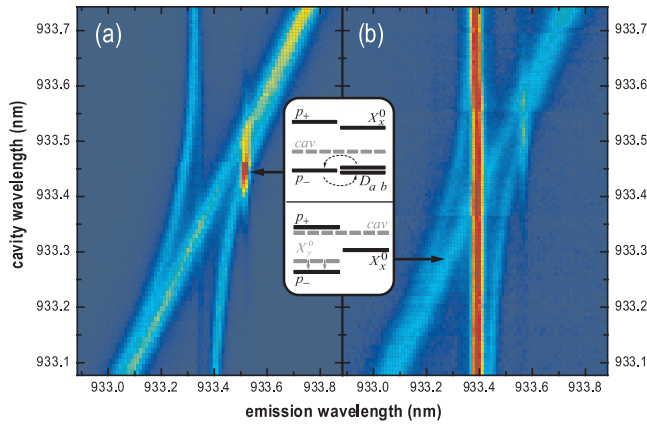


FIG. 3 (color). Comparison of X^0 dynamics for different emission polarization. (a) Zoomed-in version of Fig. 2 for the polarizer set in order to maximize cavity emission. The inset shows level schemes for two different positions of the cavity mode. In the lower inset the cavity is red-detuned from the X^0 . As the cavity photon energy is reduced, $|p_{-}\rangle$ moves in resonance with the dark states $|D_{a,b}\rangle$ as indicated in the upper inset. (b) Here the polarizer is set to 55° with respect to the cavity emission and the signal is plotted in a logarithmic color scale.

uncoupled cavity peak as in the anticrossing features observed on the X^+ and X^0 lines. This supports the hypothesis that its appearance in the latter is not an intrinsic feature of the resonantly coupled QD-cavity system itself, but rather a manifestation of off-resonant cavity feeding at times when the QD occupies a charging state other than the one the cavity is resonantly coupled to.

In comparison to the anticrossing observed on the X^+ line, the resonant signature on the X^0 shows additional features. First we notice that there is a weak additional emission line that does not shift as the cavity is tuned across resonance. This emission can be attributed to the uncoupled state $|X_x^0, 0_c\rangle$, the dipole of which is orthogonal to the cavity electric field such that it does not interact with the cavity mode. Further evidence comes from the polarization behavior of the emission: as the polarizer in the detection path is rotated, the emission from this central line increases and dominates the spectrum when oriented orthogonal to the cavity mode emission. Figure 3 shows a zoom-in of the X^0 strong-coupling feature for two different polarizations. In Fig. 3(a) the polarizer is oriented parallel to the cavity polarization, whereas in 3(b) it is rotated by 55° , in order to make emission from both the uncoupled exciton and the polariton features visible in the same spectrum.

A corresponding fine structure can be observed on the biexciton line, in that the anticrossing induced by vacuum Rabi splitting of the X^0 is only observed for a polarization parallel to the cavity mode (not shown in Fig. 3). The other pathway of biexciton decay leads through the intermediate uncoupled state $|X_x^0\rangle$. Therefore we also observe an x -polarized uncoupled biexciton line that does not shift as the cavity mode is tuned. The presence of uncoupled exciton and biexciton lines for x -polarized PL, along with the correlated anticrossings of the y -polarized X^0 and XX^0 emission lines make the identification of these transitions unambiguous.

We note that the behavior of the X^0 line differs significantly from that of the X^+ line. In particular, there is no uncoupled exciton for the latter, as expected for a charged exciton state: due to the zero total hole-spin projection in the initial state of the X^+ decay, no exchange splitting occurs. The two possible initial electron spin configurations then lead to degenerate circularly polarized transitions, either of which couple with equal strength to the cavity field. As their decay mainly proceeds via the cavity mode, the emission is copolarized with the cavity mode for both initial states. Experimentally, we confirmed that there is no uncoupled X^+ line by observing identical anticrossing features of different intensity in both polarization channels.

As tuning proceeds further to the red side of the X^0 line, an unexpected feature appears in the PL. At $\lambda_0 = 933.52 \text{ nm}$ an additional line becomes activated as the lower polariton branch $|p_{-}\rangle$ moves in resonance. We can

rule out the possibility that this line arises from a further charge configuration of the QD, since it shows a pronounced maximum for a resonance condition with the lower polariton state rather than the uncoupled cavity mode. This suggests that the mechanism responsible for inducing this luminescence stems from the excitonic component of the polariton state $|p_{-}\rangle$.

We argue that this PL peak is due to neutral dark excitons, activated by a combination of strong-coupling induced resonance with the $|p_{-}\rangle$ state and an efficient elastic spin-flip process. As the lower polariton state $|p_{-}\rangle$ is redshifted due to level repulsion, it approaches the doublet of dark excitons $|D_{a,b}\rangle$; the large cavity-exciton coupling ensures that the $|p_{-}\rangle$ state has a substantial excitonic component when it reaches exact resonance with the dark exciton transition, which occurs for a cavity wavelength of $\lambda_{\text{cav}} = 933.45$ nm [18]. A sketch of this situation is given in the insets of Fig. 3. The splitting between bright and dark exciton lines is found to be $\delta_0 = 256$ μeV , in good agreement with values reported elsewhere [19]. Furthermore, we have independently determined δ_0 from the splitting of the double negative charged exciton X^{2-} and the single negative charged biexciton $2X^{-1}$ as proposed in [20]. We identify those lines from their spectral locations and their power dependencies and determine a splitting of 0.17 nm, in close agreement to the measurement presented here.

In the off-resonant excitation scheme employed in our PL measurement, bright and dark excitons are populated with comparable probabilities, as carriers of random spin are injected into the QD. Optical decay of the population stored in the dark excitons however requires a spin-flip to take place prior to the optical recombination event. The strong dependence of the dark exciton PL on the detuning from the lower polariton branch observed here suggests that an elastic spin-flip process is involved in the optical activation of dark exciton decay. A strong candidate mechanism is the hyperfine interaction between the electron in the QD and the spins of the lattice nuclei. In this process angular momentum can be exchanged with negligible energy transfer [21]. For QDs outside a cavity this process is very inefficient, since the exchange energy δ_0 has to be overcome in order to flip the electron spin. However, as δ_0 is compensated by the strong-coupling induced shift of $|p_{-}\rangle$, we expect a significant increase of the hyperfine induced electron spin-flip rate.

Typical hyperfine interaction strengths are on the order of $\Omega_N \approx 0.5$ μeV for QDs with $\approx 10^5$ atoms [21]. The effective optical recombination time of dark excitons via the resonant intermediate lower polariton state $|p_{-}\rangle$ then is given by $\gamma_p/\Omega_N^2 \approx 110$ ns, where γ_p is the linewidth of the lower polariton. This time scale is relatively long compared to the < 100 ps time scale of polariton recombination and the ≈ 10 ns time scale of the uncoupled exciton within the photonic bandgap. However, both bright and dark ex-

citons are created with equal probability in the QD, such that the populations of the two are comparable for pump powers well below saturation. Even for different decay times this leads to comparable PL intensities of the cavity-induced dark exciton luminescence and the PL from the polariton states, which we confirm by multi-Lorentzian fits to our data. We note that as the pump power is increased, the dark excitons can make transitions to other charge configurations by the capture of additional carriers, which results in a depletion of the dark exciton population. Indeed we have verified this from power dependent measurements on a control device.

In conclusion we show that the strong-coupling limit of cavity QED can be used as a powerful spectroscopic tool, providing an unambiguous identification of QD spectral features. Our findings could prove to be useful in more complicated systems such as coupled-QDs where the multitude of emission lines render precise identification of PL lines more difficult.

The authors would like to acknowledge Andreas Reinhard for helpful discussions. This work is supported by NCCR Quantum Photonics (NCCR QP), research instrument of the Swiss National Science Foundation (SNSF).

*wingerm@phys.ethz.ch

- [1] H. Mabuchi and A. C. Doherty, *Science* **298**, 1372 (2002).
- [2] J. M. Raimond, M. Brune, and S. Haroche, *Rev. Mod. Phys.* **73**, 565 (2001).
- [3] P. Michler *et al.*, *Science* **290**, 2282 (2000).
- [4] A. Imamoglu *et al.*, *Phys. Rev. Lett.* **83**, 4204 (1999).
- [5] T. Yoshie *et al.*, *Nature (London)* **432**, 200 (2004).
- [6] E. Peter *et al.*, *Phys. Rev. Lett.* **95**, 067401 (2005).
- [7] J. P. Reithmaier *et al.*, *Nature (London)* **432**, 197 (2004).
- [8] K. Hennessy *et al.*, *Nature (London)* **445**, 896 (2007).
- [9] D. Englund *et al.*, *Nature (London)* **450**, 857 (2007).
- [10] K. Srinivasan and O. Painter, *Nature (London)* **450**, 862 (2007).
- [11] L. C. Andreani, G. Panzarini, and J.-M. Gerard, *Phys. Rev. B* **60**, 13 276 (1999).
- [12] A. Badolato *et al.*, *Science* **308**, 1158 (2005).
- [13] Y. Akahane *et al.*, *Nature (London)* **425**, 944 (2003).
- [14] M. Bayer *et al.*, *Phys. Rev. B* **65**, 195315 (2002).
- [15] E. L. Ivchenko, *Phys. Status Solidi A* **164**, 487 (1997).
- [16] G. Bester, S. Nair, and A. Zunger, *Phys. Rev. B* **67**, 161306 (R) (2003).
- [17] S. Strauf *et al.*, *Appl. Phys. Lett.* **88**, 043116 (2006).
- [18] We note that the PL enhancement is not symmetric around the dark exciton resonance. This asymmetry is probably due to the increasing linewidth of the lower polariton as it crosses the resonance.
- [19] R. M. Stevenson *et al.*, *Phys. Rev. B* **73**, 033306 (2006).
- [20] B. Urbaszek *et al.*, *Phys. Rev. Lett.* **90**, 247403 (2003).
- [21] I. A. Merkulov, A. L. Efros, and M. Rosen, *Phys. Rev. B* **65**, 205309 (2002).